

Time Resolved Fluorescence Anisotropy of Combustion Generated Nanoparticles *Ex Situ* and *In Situ*

A. Bruno^{1,2}, P. Minutolo⁴, C. de Lisio^{1,2}, N. Spinelli¹, A. D'Alessio⁵

1. Dipartimento di Scienze Fisiche- Università Federico II, Napoli - ITALY
2. Centro di Ricerca e Sviluppo "Coherentia", C.N.R. – I.N.F.M., Unità di Ricerca di Napoli
3. Division of Combustion Physics –Physics Department -Lund University- SWEDEN
4. Istituto di Ricerche sulla Combustione - C.N.R., Napoli – ITALY
5. Dipartimento di Ingegneria Chimica - Università Federico II, Napoli – ITALY

In this work we report on the analysis of combustion-generated nano-organic carbon (NOC) particles by means of time-resolved fluorescence polarization anisotropy (TRFPA). The analysis has been applied on NOC samples collected in water from non-sooting regions of ethylene/air laminar flames and directly in a Bunsen-type propane flame. In both cases presence of very small fluorescing particles has been shown.

The results of this work strongly support the attribution of UV/Visible fluorescence detected in flames to nanoparticles. These results also evidence that NOC nanoparticles undergo a chemical transformation during the growth process which produces a red shift in the fluorescence spectrum.

1. Introduction

Recent studies have identified in rich premixed flames a large variety of carbon nanoparticles, ranging from smaller ones, with sizes smaller than 3 nm and defined as nanoparticles of organic carbon (NOC), to larger soot particles with typical size of 20 nm and more, up to micron for the aggregates of primary particles.

In situ optical diagnostics like UV-visible absorption, elastic light scattering (D'Alessio, 1992; D'Anna, 1994; Minutolo, 1998), fluorescence spectroscopy (Minutolo, 1999) have been previously applied. Also *ex-situ* techniques have been employed for the characterization of NOC (Sgro, 2001.), such as light absorption and fluorescence, atomic force microscopy (AFM) (Barone, 2003), dynamic light scattering (DLS) (Cecere, 2003), differential mobility analysis (DMA) (Sgro, 2003), and Infrared absorption (Rusciano, 2006).

Fluorescence is a very specific indicator of chemical species and can be employed in structured media with excellent time and spatial resolution. Its main limit is that normally it does not allow a simultaneous determination of the molecular mass of the emitter which contains the chromophore group.

This problem is overcome when fluorescence emission is induced by ultrafast light excitation, much shorter than the typical fluorescence lifetime. In this case the polarization decay which is due to the rotation of the structure, can be followed and related to the nanoparticles size. This method defined as Time Resolved Fluorescence Polarization Anisotropy (TRFPA) has been employed in the field of proteins and more recently it has been applied to nanoparticles in combustion systems.

TRFPA measurements and analysis open up for a new field of size and, to some extent, spectral characterization of fluorescent nanoparticles. A detailed description of the technique and some recent improvements are reported in Ref (Lakowicz , 2002) and reported briefly in next paragraph.

This communication summarizes the principles, discusses the application of the method to the onset of carbon nanoparticles formation in premixed laminar flames (*ex-situ* measurements) and outlines its potentialities in laminar diffusion flames (with *in-situ* measurements). Finally, some speculation on the application of this diagnostics to more complex situation in the exhaust of combustion systems and in the urban atmosphere is advanced.

2. Time Resolved Fluorescence Polarization Anisotropy

The phenomenon of fluorescence polarization anisotropy is characterized by the time-dependent anisotropy ratio, $r(t)$, defined as:

$$r(t) = \frac{I_{\parallel}(t) - I_{\perp}(t)}{I_{\parallel}(t) + 2I_{\perp}(t)}. \quad (1)$$

$I_{\parallel}(t)$ and $I_{\perp}(t)$ represent the intensities of parallel and orthogonal components of fluorescence light. In the simplest case of a spherical rotator, the anisotropy ratio decays with a single exponential function (Lakowicz , 2002):

$$r(t) = r_0 \exp\left(-\frac{t}{\tau_{rot}}\right), \quad (2)$$

where τ_{rot} is the characteristic rotational time of the fluorescing particles and r_0 is the initial value of r . The quantity τ_{rot} depends on the rotational diffusion coefficient D_r , and, in turn, on the volume, V , of the diffusing particle through the Stokes-Einstein-Debye equation:

$$\tau_{rot} = \frac{1}{6D_r} = \frac{\eta V}{k_B T}, \quad (3)$$

where T and η are, respectively, temperature and viscosity of the suspension. From the volume V , the radius of a volume equivalent sphere, defined as the particle hydrodynamic radius, R_{hy} can be easily determined.

By analysing the time evolution of $r(t)$, it is possible to determine τ_{rot} and so knowing temperature and viscosity of the sample, estimate R_{hy} of fluorescing particles.

This technique is also capable to determine the dimensions of various particle in a polydispersed sample, when particles with different size also have different spectral properties. This can be achieved by exploiting wavelength selectivity in both absorption and emission processes: following excitation at a fixed wavelength, fluorescence

emission from different groups of particles will generally occur at different wavelengths. Consequently, by limiting the TRFPA analysis to a restricted fluorescence band, it is possible to determine the characteristic size of particles emitting in the selected wavelength band.

For a gaseous environment at high temperature like the flame, where the viscosity is much lower, the rotational correlation time, and consequently the fluorescence depolarization rate are affected in addition to the medium viscosity, by the momentum of inertia of the particles moving as free rotator. In these conditions, it can be shown that the dynamic of the rotational process can be described by a Langevin type equation in the diffusive limit of the rotational correlation time. On the contrary, the initial particle reorientation, at short initial times, occurs in a regime of coherent initial motion and the particle motion has not yet been influenced by the surrounding gas. In this case the anisotropy is described by:

$$r(t) = r_0 \exp\left[-\frac{3k_B T}{M} t^2\right],$$

In such a case, the time profile of the anisotropy matches the early time behaviour of free rotational motion described by a Gaussian (Bruno, 2008).

3. Experimental

The laser system (Spectra Physics) used as excitation source for TRFPA measurements consisted of a mode-locked Titanium:Sapphire (Ti:Sa) laser (model Tsunami) amplified by a Ti:Sa amplifier (model Spitfire) delivering pulses with a maximum energy of 0.6 mJ at $\lambda \approx 800$ nm, 100 fs duration and 1 kHz repetition rate. The 2nd and the 3rd harmonics at 400 and 266 nm respectively, were used for the TRFPA experiments. The detection system consisted of: a polarizer (to select vertical and horizontal components of fluorescence); a transmission wavelength-selective filter; and a photomultiplier tube (PMT, Hamamatsu: H6780) with fast response time of 0.6 ns. The signals from the PMT were recorded by 2 GHz bandwidth oscilloscope (Tektronix: TDS794) (Bruno, 2005). The optical scheme employed for the in situ measurements is similar to the *ex-situ* one. The measurements were performed using just the output from the laser oscillator delivering linearly polarized radiation of 10 nJ energy/pulse at repetition rate of 82 MHz. The laser oscillator was optimized to produce laser wavelength at about 760 nm. The second harmonic of the fundamental radiation (380 nm) was focused into the centre of a 1 cm Bunsen burner. Pure propane was used as combustible gas. The detector was a streak camera mode with 5 ps resolution. The fluorescence signal was averaged over 2,000 events (Bruno, 2008).

4. Results

4.1 Ex situ measurements

We report the analysis of NOC particles collected from ethylene/air laminar flames generated in water-cooled McKenna burner with combustible/oxidant (C/O) ratios from C/O=0.56 to 0.69. The combustion products of these flames were collected using a stainless steel, water cooled probe bubbled through bi-distilled water. For more details on the sampling procedure see Ref (Sgro, 2001)

Figures 1 a) and b) show the fluorescence spectra for excitation wavelengths of 266 nm and 400 nm, respectively. It is noteworthy that the overall shape of the spectra was almost independent of the C/O ratio. When the samples were excited at 266 nm (Fig. 1 a)), all spectra presented two broad bands, the first centred around 310 nm and the second one, less intense, extending in the visible region from 390 to 500 nm. Superimposed onto the broad emission, a few small but sharper peaks appeared at the wavelengths of 341, 355 and 370 nm that can be attributed to small contribution of free PAHs. When the same samples were excited at 400 nm presented a wider fluorescence profile extending up to 650 nm, with the maximum around 480 nm (Fig. 1(b)). The samples showed the same spectroscopic features observed with *in situ* measurements in the corresponding flames (see Ref (Minutolo, 1999) for comparison)

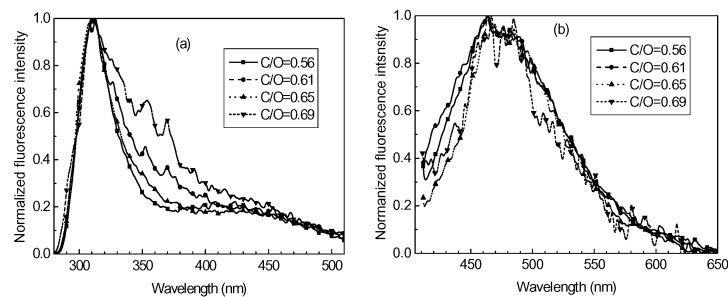


Figure 1: Normalized background corrected fluorescence spectra for water suspensions of samples collected from ethylene/air flames with different C/O ratios, obtained with excitation wavelengths of 266 nm (a) and 400 nm (b).

The hydrodynamic diameters of the sampled particles were measured by TRFPA with excitation at both 266 nm and 400 nm and selecting different fluorescence wavelengths within the fluorescence band. The experimental results are summarized in Fig. 2, where the measured particle sizes are plotted as a function of the emission wavelength. Similar trends were observed for different C/O ratios, indicating that the composition of the samples was substantially the same. In particular, we can infer that the samples mainly consisted of two types of particles, one fluorescing in the spectral range below 470 nm having an average size of about 1.5 nm, and the other emitting above 470 nm being larger than 2 nm (Bruno, 2005).

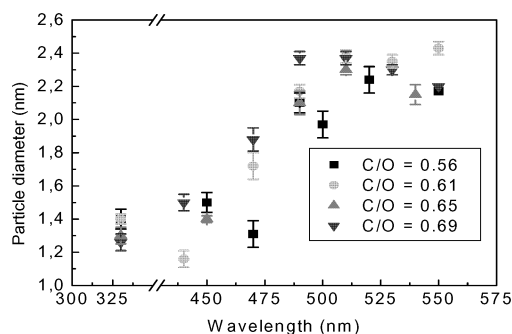


Figure 2: Diameters of water suspended particles collected from different C/O ratio flames, as a function of the emission wavelength. Results were obtained with excitation wavelength of 400 nm, except data points at 330 nm, obtained with 266 nm excitation wavelength.

The red shift of the peak emission of the larger particles, may be explained by the presence of larger aromatic groups, with more than three condensed rings, inside the particles while the UV fluorescing smaller particles probably contain aromatic groups made of one-,two, benzenic rings. However, we cannot rule out that this class of particles is formed from the aggregation of 3–4 of the smaller UV fluorescing particles, a process which would give rise to the delocalization of π -electrons over a larger volume.

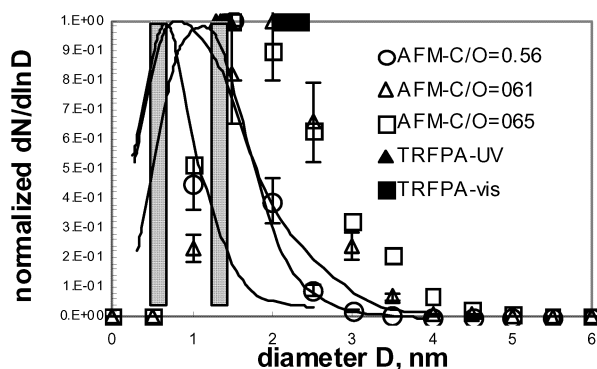


Figure 3: Normalized particle size distribution function measured by AFM, on particles collected from flames with various C/O ratio and corrected for the size dependent stiking efficiency. TRFPA measured in the UV and the visible are also reported and a gray zone is reported to indicate the range of data variation with C/O ratio.

In order to investigate the possible role of water, in which particles are suspended, in creating particle aggregate, we have compared TRFPA results with the Particle Distribution function, PDF, measured by Atomic Force Microscopy, AFM, on particles collected from the same flames by thermophoretic sampling on mica plates adapted from Sgro et al. 2008. AFM and TRFPA results are reported in fig. 3.

The PDF measured in flames with $C/O=0.56-0.65$ are quite similar with a maximum around 2 nm. TRFPA results are well within the AFM-PDF. The smaller UV fluorescing particles are close to the modal value of PDF measured in the less rich flame, $C/O=0.56$, while the larger particles constitute the upper tail of the PDF which is larger in the richer flames.

These results seem to exclude that aggregate are produced into the water samples, but it will be definitely ruled out by performing in flame TRFPA measurements. Such measurements are very difficult because of the high temperature environment and only preliminary measurements have been performed in a Bunsen type flame.

4.2 In situ measurements

Figure 4 shows the two polarization components, $I_{\parallel}(t)$ and $I_{\perp}(t)$, of the fluorescence intensity collected from the centre of a Bunsen type flame as a function of time. In the same figure we also report the time profile (multiplied by a factor of 100) of the laser radiation scattered from air. The latter is assumed as the instrument response function of our apparatus.

The anisotropy ratio derived from Eq. (1) is reported in the inset of Fig. 4, where the time origin has been shifted, so that $t = 0$ corresponds to the maximum of $r(t)$. The time profile of the anisotropy clearly presents two distinct regions: During the first 50 ps it follows a Gaussian behaviour, as expected in case of free coherent rotation, whereas at long times, a nearly exponential decay can be observed, although overlapped to a rather large noise.

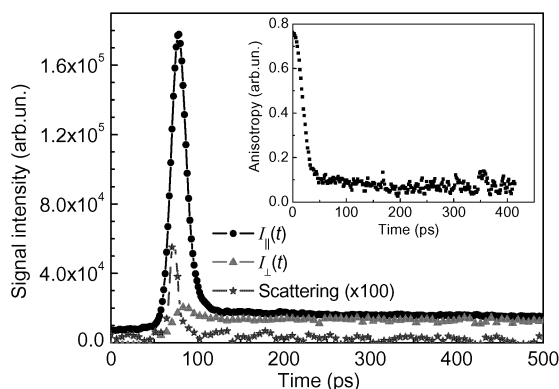


Fig. 4. Signal intensities of $I_{\parallel}(t)$ (black dots), $I_{\perp}(t)$ (red triangles), and scattering signal

An expanded view of the first 80 ps of the anisotropy ratio is reported in Fig. 5, where the red line is a Gaussian fit. For NOC particles in the propane flame conditions ($\rho = 10^3 \text{ kg/m}^3$, $T = 885 \text{ K}$), we obtained an average particle diameter, D , of $(3.3 \pm 0.3) \text{ nm}$. The uncertainty must not be interpreted as the particle size-distribution width, which cannot be determined with our present experimental setup and data analysis. It is the maximum deviation of the estimate of D and is related to the standard deviation of the Gaussian time width ($\cong 3\%$) and to maximum deviations of T and ρ , both of about 15%. The above result confirms the initial assumption of carbon particles with dimensions of a few nanometres, although we cannot rule out that NOC

particles have a non-spherical shape. However, besides particles' shape and size distribution, our results unambiguously prove that the propane flame does produce small nanoparticles, showing a significant emission at wavelengths around 420 nm and dimensions shorter than 4 nm. As an additional relevant result, we have demonstrated that the TRFPA technique lends itself to the physical characterization of nanometric carbon particles directly within the flame, thus eliminating sampling and subsequent *ex situ* analysis. This feature allows a more direct characterization of the flame products, removing both the need of a collecting probe, that could alter the combustion process, and dilution of the collected particles in a solvent, which can modify the particles' characteristics. Moreover, the method can be easily applied to flames and combustion systems where sampling is either difficult or unsuitable (*e.g.*, counter-flow diffusion flames).

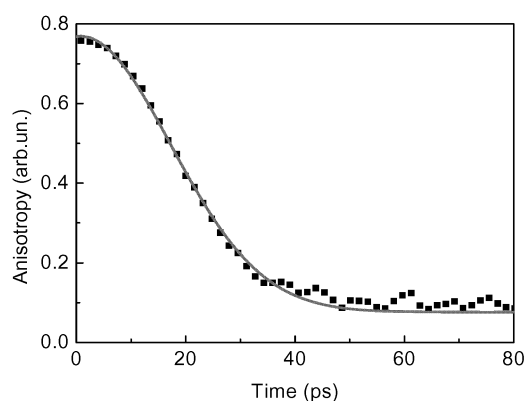


Figure 5. Time behaviour of anisotropy at the early time

5. Conclusions

In this work we report on the description of the *ex situ* and *in situ* implementation of TRFPA. The idea is to demonstrate that fluorescence signals detected in flame and in water samples originate not only from small molecules like PAH but also from NOC nanoparticles. The size composition of water-suspended NOC particles sampled from non sooting and slightly sooting ethylene-air premixed flames have been determined using a spectrally resolved TRFPA analysis. In particular, the NOC samples consisted of two groups of particles, preferentially emitting in two distinct wavelength bands: smaller particles, $d=1-1.5$ nm fluoresce mostly in the UV, $\lambda\sim 300-470$ nm, while larger particles, $d>2$ nm exhibit a red shift in the fluorescence spectrum, $\lambda\sim 490-580$ nm. Then we have also performed *in situ* application of TRFPA to the detection of nanoparticles in a propane Bunsen-type diffusion flame. For the flame condition analyzed very small particles have been detected. The preliminary results reported in this work strongly support the attribution of the fluorescence detected in flames to NOC particles. Further work in well characterized premixed flame are in progress in order to infer information on the chemical transformation of the particles during the kinetics process of particles growth and soot inception.

6. Refences

- Barone, A.C., D'Alessio, A., D'Anna, A., 2003, *Combustion and Flame* 132, 181.
- Blokhin, A.P., Grelin, M. F, Buganov, O. V., Dubovskii, V. A., Tikhomirov, S. A., and Tolstorozhev, G. B., 2003, *Journal of Applied Spectroscopy*, 1, 70.
- Bruno, A., Minutolo, P., de Lisio, C. , 2005, *Opt. Express* 13, 5393.
- Bruno, A., Ossler, Frederick, Minutolo, P., de Lisio, C., Spinelli, N, D'Alessio, A, 2008, *Opt. Express* 16, 5623-5632.
- Cecere, D, Bruno, A., Minutolo, P., D'Alessio, A. , 2003, *Synthetic Metals* 139, 653.
- D'Alessio, A., D'Anna, A., D'Orsi, A.P., Minutolo, Barbella, R. Ciajolo, A., 1992, *Proceedings of The Combustion Institute* 24, 973.
- D'Anna, A., D'Alessio, A., Minutolo, P. : H. Bockhorn, Eds, 1994, *Soot Formation in Combustion: Mechanisms and Models of Soot Formation*, Springer-Verlag, Berlin
- D'Anna, A., Roando, A, Allouis, C., Minutolo, P., D'Alessio, A., 2005, *Proceedings of The Combustion Institute* 30, 1449
- Lakowicz, J.R., *Principles of Fluorescence Spectroscopy*, 2002 Kluwer Academic/Plenum Publisher, New York.
- Minutolo, P. , Gambi, G., D'Alessio, A., 1998, *Proceedings of The Combustion Institute* 27, 1461
- Minutolo, P., Gambi, G., D'Alessio, A., Carlucci, S., 1999, *Atmos. Environ.* 33, 2725
- M.M. Maricq, 2005 *Combust. Flame* 24, 406.
- Rusciano, G., Cerrone, G., Bruno, A., Minutolo, P., Sasso, A.: 2006, *Appl. Phys. B*, 82, 155.
- Sgro, L.A., Minutolo, P., Basile, G., D'Alessio, A., 2001, *Chemosphere* 42, 671.
- Sgro L.A., G. Basile, A.C. Barone, A. D'Anna, P. Minutolo, A. Borghese, A. D'Alessio, 2003, *Chemosphere* 51, 1079.
- Sgro, Lee A, Borghese, A, Speranza, L, Barone, AC , Minutolo, P, Annalisa Bruno, A, D'Anna, A, D'Alessio A, 2008, *Environ. Sci. Technol.*, 42 , 859.
- Zhao B., Z. Yang, M.V. Johnston, H. Wang, A.S. Wexler, M. Balthasar, M. Kraft, 2003, *Combust. Flame* 133, 173.
- Zhao B., Z. Yang, Z. Li, H. Wang, 2004, *Proc. Combust. Inst.* 30, 1441.